Project Title:

Nucleon Structure from Lattice QCD with Domain Wall Fermions

Name: ○Meifeng Lin(5)(1), Tom Blum(2)(1), Taku Izubuchi(4)(1), Chulwoo Jung(4)(1), Shigemi Ohta(6)(7)(1), Shoichi Sasaki(8)(1), Takeshi Yamazaki(9)(1)

Laboratory at RIKEN:

(1) RIKEN BNL Research Center, Upton, New York, USA
(2) Department of Physics, University of Connecticut, Storrs, Connecticut, USA
(3) Department of Physics, University of Virginia, Charlottesville, Virginia, USA
(4) Physics Department, Brookhaven National Laboratory, Upton, New York, USA
(5) Computational Science Center, Brookhaven National Laboratory, Upton, New York, USA
(6) Institute of Particle and Nuclear Studies, KEK, Tsukuba, Japan
(7) Department of Particle and Nuclear Physics, Sokendai Graduate University of Advanced Studies, Hayama, Kanagawa, Japan
(8) Department of Physics, Tohoku University, Japan
(9) Center for Theoretical Studies, Nagoya University, Japan

Description of the project

1. Introduction

1.1 Scientific Background

Protons and neutrons (collectively called nucleons) compose the major part of atoms, and are fundamental building blocks of matter. Understanding their internal structure advances our fundamental knowledge about the composition of the universe. Many particle and nuclear experiments worldwide are actively probing the charge, current, magnetization and other fundamental properties of protons and neutrons, such as Mainz in Germany and the Jefferson Lab in the US. In particular, RHIC-Spin experiment at Brookhaven National Laboratory in the US probes the spin structure of the nucleon. From a theorist's point of view, being able to interpret the observed experimental data and predict new properties of the nucleons from first-principles theories enhances our fundamental understanding of the underlying interactions and is the ultimate goal of our proposed research topic.

The theory that describes the interactions inside a proton is the so-called "Standard Model" of particle physics. In particular, we will be interested in the component of the Standard Model known as Quantum Chromodynamics (QCD). In this theory, a proton consists of "quarks" which are fermions with fractional charges, and "gluons" which mediate the strong interactions among quarks. Because of the nature of the strong interactions, traditional perturbative theoretical calculations (which assume that fermions receive only small corrections to their behavior from the force carrying bosons) fail to work. In the 1970s Kenneth Wilson (later to win the Nobel Prize for his work on the Renormalization Group and Critical Phenomena) formulated Lattice QCD [1]. This did two things: firstly, it provided a rigorous definition of the meaning of QCD beyond perturbation theory, and secondly it provided a way to perform first-principles calculations numerically. While it has taken several decades of improvements in computing power and algorithmic developments, recently the latter has been very successful in reproducing observed experimental data, such as the particle spectrum and decay properties. In lattice QCD calculations, the four-dimensional space-time is discretized into a box with discrete grid points and Monte Carlo simulations based on the Standard Model are carried out on computers. Since lattice QCD simulations are carried out in a finite box, at finite quark masses and at a finite lattice spacing, before we can reliably interpret our results, we need to have the associated systematic errors under control.

The two most prominent systematic errors may be the errors associate with the finite volume and finite quark masses in the lattice calculations. In order to relate the results from lattice simulations to the real world, extrapolations are required to obtain results at the physical point which can then be compared to known experimental values or as predictions for future experiments. Chiral perturbation theory (ChPT) [2], a low-energy effective theory, is often used to guide the extrapolation. However, at the order practical for our calculation, chiral perturbation theory is only applicable at small quark masses (or equivalently, small pion masses). Existing lattice calculations of nucleon structure have pion masses only as low as 300 MeV (while the physical pion mass is about 135 MeV), which are at the edge of the applicability of chiral perturbation theory of the appropriate order. It has been found [3] that lattice results at these pion masses are not consistent with the predictions of chiral perturbation theory, and the extrapolated values using ChPT deviate from the experimental values, indicating the

systematic errors from chiral extrapolations are large. Doing lattice calculations at lighter pion masses will greatly reduce the uncertainty associated with the chiral extrapolation and has the potential to produce high-precision results valuable to both the theory and experiment communities.

As the pion mass gets lighter, the pion Compton wavelength gets larger, and the size of the lattice volume needs to be larger to accommodate the pions. As the pion mass gets lighter and the volume gets larger, the numerical cost of the lattice calculations increases dramatically. Due to the complexity, and expense, of such calculations, there are naturally large research collaborations to facilitate the research efforts.

The RIKEN-BNL-Columbia (RBC) collaboration started around the same time as the RIKEN-BNL Research Center (RBRC) was founded in 1997. RIKEN and Columbia jointly built the 600-GFlops QCDSP (Quantum Chromodynamics on Digital Signal Processors) computer dedicated for lattice-QCD numerical research at RBRC. The RBC also pioneered the use of a particular formulation of lattice QCD known as Domain Wall Fermions (DWF) [4,5]. Traditional lattice discretizations break many of the symmetries of the continuum theory. Perhaps the most important of these is "chiral symmetry" which says that "left-handed" and "right-handed" quarks are only coupled due to the small mass terms of the quarks. Naive lattice QCD formulations lead to couplings which are orders of magnitude too large. In DWF an additional fifth dimension is introduced to the space-time, with the left- and right-handed fermions living on opposite four-dimensional boundaries of the five-dimensional space, which greatly improves chiral symmetry. This formulation revolutionized the way numerical lattice QCD research is conducted. An important outcome was that the so-called non-perturbative renormalization [6] method became practical, and made possible, for the first time in history, accurate calculations of quantum transitions between hadronic states.

1.2 Research Purpose

The purpose of this multi-year project is to calculate the structure of nucleons using lattice QCD techniques. The primary focus of this research is to calculate all the isovector vector- and axial-vector form factors and some low moments of isovector structure functions of nucleon using a new set of lattice QCD numerical ensembles at larger than ever spatial volume of about 4.5 fm across and pion masses as low as 170 MeV [7]. An exploratory study of the nucleon strangeness content will also be pursued. We also use a small fraction of the time for algorithmic developments. Detailed descriptions of each topic are given below.

(1) Precision lattice determination of nucleon mass. Being able to reproduce the experimentally well-known nucleon mass from the first-principles lattice calculations is a first step in establishing the precision test of lattice QCD. Previously, the heavy pion masses in the calculations make it hard to perform chiral extrapolations. With nearly physical pion mass in our calculations, we will be able to obtain a nucleon mass which is free of large systematic errors coming from chiral extrapolations. We will also be able to investigate the validity of chiral perturbation theory in these small pion mass ranges. Such calculations will be a great milestone towards high-precision lattice calculations.

(2) Nucleon vector form factors. Nucleon isovector vector form factors are part of the electromagnetic form factors and thus studied mainly by elastic electromagnetic processes such as electron scattering off nucleons or nuclei. They provide information of such important properties as mean-squared charge radii or anomalous magnetic moments which determine electromagnetic interactions of nuclei with other electromagnetic entities such as photon and electron. Thus these form factors ultimately determine electromagnetic properties of atoms which in turn govern properties of chemistry and biology.

Because the quark masses in lattice calculations are heavier than reality, extrapolations that utilize the formula given by chiral perturbation theory are needed. In order to be able to reliably apply the chiral formula, the quark masses in the simulations need to be small enough. Previous lattice calculations have pion masses usually larger than 300 MeV, while a physical pion mass is about 140 MeV, which requires a long extrapolation from the simulated data to the physical point. Performing lattice calculations on the new DWF ensembles at pion masses of 250 MeV and 170 MeV will significantly reduce the systematic errors coming from chiral extrapolations. In addition, the large volume of the new ensembles will make the calculations less susceptible to finite volume effects and have the potential of achieving unprecedented statistical and systematic precisions.

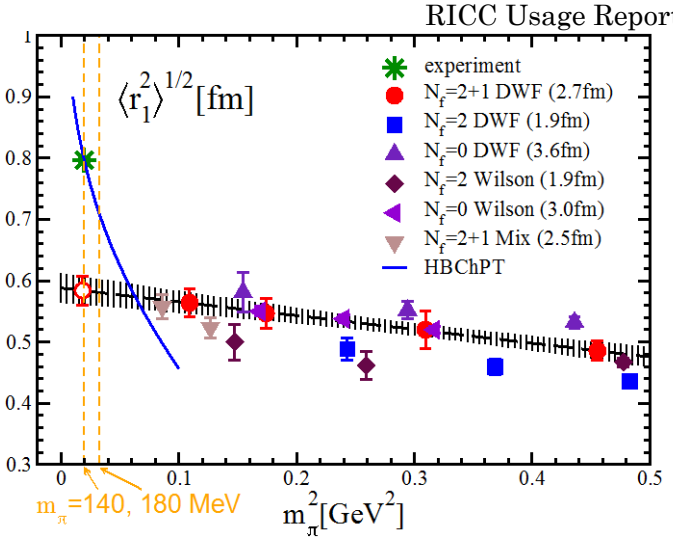

Figure 1: Nucleon isovector charge radii from previous lattice calculations. The green star is the experimental point, and the blue curve is prediction from chiral perturbation theory.

Given in Figure 1 are the results from previous lattice calculations [8] for the nucleon isovector Dirac radii as a function of the pion mass squared, where the lattice results are systematically lower than the experimental point and are not consistent with the prediction from chiral perturbation theory. A naive linear extrapolation to the lattice data gives a value at the physical point which is much smaller than expected. Having lattice results at lower pion masses will undoubtedly improve our ability to perform a more reliable chiral extrapolation.

(3) Nucleon axial form factors. Nucleon axial and induced pseudoscalar form factors probe the weak structure of the nucleon, and are also actively pursued experimentally, for example by using muon instead of electron: muon capture process is sensitive to a part of these form factors, g_P, for example.

The nucleon axial charge g_A is defined as the zero momentum-transfer limit of the axial form factor, and determines the neutron lifetime. It is indeed best measured in neutron beta decay, in which a neutron decays into a proton via weak interaction and emits an electron and anti-neutrino. It also controls the interaction of pion and nucleon through the Goldberger-Treiman relation. Thus it is the single most important nucleon property in determining the abundance of elements that are formed in premordial and stellar nucleosynthesis. In contrast to the corresponding vector charge, g_V, which is not affected by the strong interaction, it receives corrections from the strong interaction and deviates from unity in units of g_V, $g_A = 1.2701(25)\ g_V$. We recently discovered this strong correction is strongly dependent on the pion mass and the volume in which the lattice calculation is conducted [9]. This is shown in Figure 2, where lattice results from different lattice volumes and different lattice formulations depend not only on the pion masses, but also the volumes. Our current calculations will continue to explore the dependence of g_A on the pion mass and the lattice volume, and allow us to perform a more reliable extrapolation to obtain a physical value for g_A.

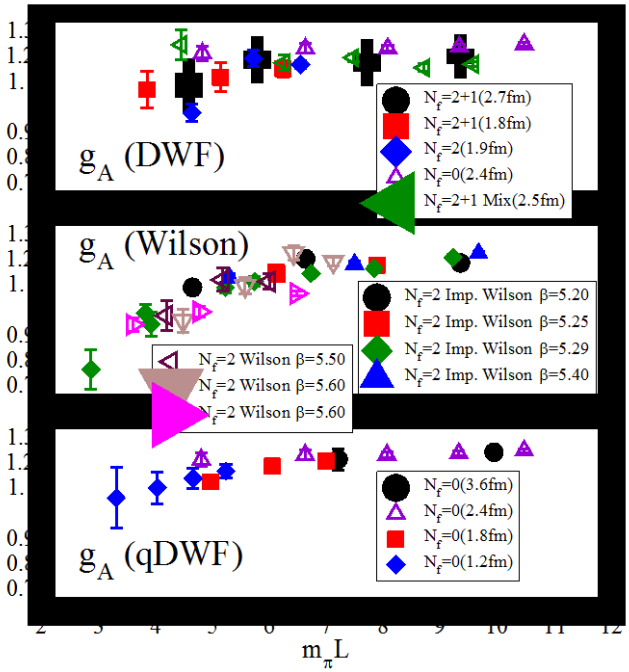

Figure 2: $m_\pi L$-scaling for g_A, which indicates finite volume effects.

(4) Nucleon structure functions. Studied mainly by lepton deep inelastic scattering and Drell-Yan experiments off nucleon and nuclei, these reveal deeper structures of nucleon and led to discovery of quarks and QCD. RIKEN experimenters are trying to resolve a puzzle in spin-dependent structure functions of nucleon through the RHIC-Spin experiments now conducted at RIKEN-BNL Research Center. Of particular interest are the quark momentum fraction, helicity fraction, and tensor charge, all in isovector combinations.

For the first two quantities conventional lattice-QCD numerical calculations significantly over estimate the experimental values. A recent joint study [10] by RBC and UKQCD collaborations found that at the lightest quark mass value that corresponds to 330 MeV pion mass these values trend down to the experiment. By comparing the two different volumes, it is suggested the finite-size effects in these quantities seem absent, in contrast to the situation for the axial form factors discussed in the above. It is thus interesting to see if the trend toward experiment and apparent absence of the finite-size effect hold at the lighter quark masses that correspond to 250 MeV and 170 MeV pions.

For tensor charge the same joint RBC/UKQCD study have a crude prediction. As this quantity will soon be

experimentally measured, it is obviously important to refine this prediction at lighter quark mass values.

(5) Excited-state Contaminations

In the past three years, we have performed nucleon structure calculations on the gauge ensembles described above using the RICC resources and US Teragrid/XSEDE resources. With continuously improved algorithms, we have been able to obtain results for the nucleon mass, nucleon axial charge and nucleon vector form factors with statistical errors as small as sub-1% on the 250 MeV ensemble. These results as they are already represent the forefront of the current lattice nucleon structure calculations. These observables are properties of the nucleon ground states. But the nucleon correlation functions we obtain from the simulations contain information for a tower of nucleon excited states. Only when one gets to large enough distance in time can the nucleon ground state dominate the signal. Our calculations have been done with only one separation between the nucleon source and the nucleon sink, while recent studies have indicated that several separations may be needed to eliminate the excited-state contaminations, an important source of possible systematic errors. One of such studies [11] is shown in Figure 3. Our source-sink separation of 9 lattice units is as large as the largest in their study, and may be large enough for us to ignore the effects of excited-state contaminations. when the statistical errors dominate. Now we have reached statistical errors of a few percent, which makes it necessary to carefully investigate the possible contaminations from nucleon excited states.

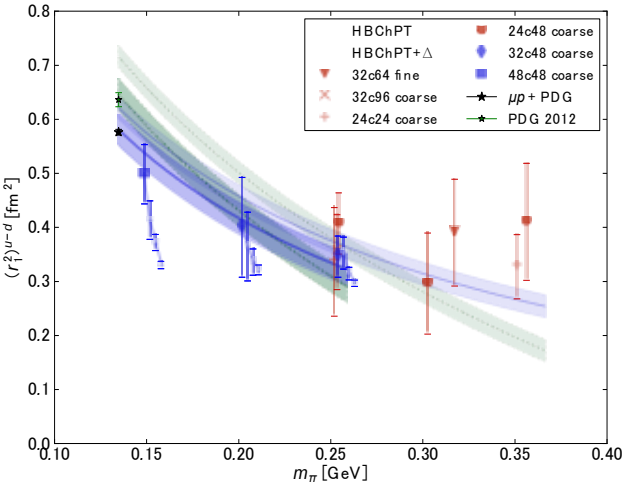

Figure 3: Studies of source-sink separations for the isovector Dirac radii. Groups of open symbols indicate, from right to left, increasing separations between nucleon source and sink. Filled symbols indicate the results with excited-state contaminations removed. Plot is from arXiv: 1209.1687.

The purpose of the FY2013 proposal was to calculate the structure of nucleons using lattice QCD techniques at a larger source-sink separation, T=11, so that excited-state contaminations can be definitively eliminated. Our aim was to achieve 3% or better statistical errors on the nucleon axial charge, 5% or better error on the nucleon vector and axial form factors and their associated root-mean-squared radii. Combined with our previous calculations of a source-sink separation of 9 lattice units, and an ongoing calculation with a smaller source-sink separation of 7 lattice units in the US, we were planning to extrapolate to infinite source-sink separation, eliminating the possible excited-state contaminations.

2. Computational Details and Usage Status

2.1 Computational Methods

We perform our calculations with domain wall fermions on the existing gauge backgrounds generated by the RBC and UKQCD collaborations [7] . These gauge backgrounds encode a particular configuration of the gluon fields. For each such configuration we need to calculate the sum of all possible paths a quark can take between a given set of starting positions (sources) and all points on the lattice. While other calculations will be involved, this will be the dominant calculation in terms of computer time. The natural unit in which to measure such things is a single starting position (source). A single starting position leads to the calculation of a single, forward, quark propagator. From each propagator four so-called sequential propagators (sink) will be needed to perform the proposed calculations. The sequential propagators will then multiply the forward propagator from the source with appropriate operators and momentum of interest to construct two and three-point functions of the nucleon. For each nucleon three-point function, 5 quark propagators (one forward and four sequential quark propagators) will be needed. Since we perform Monte Carlo simulations, we will need to do the calculations on multiple gauge backgrounds so that statistical averages and errors can be calculated.

The two-point nucleon correlation functions are traces of the products of the forward propagators, and the three-point functions are traces of the products of the forward propagators and sequential propagators. A graphical representation of the so-called connected diagram of the three-point function is shown in Figure 4.

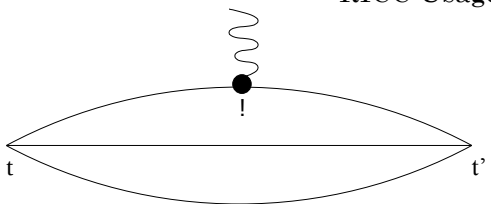

Figure 4: An illustration of the connected contribution to the nucleon three-point functions. t and t' are the locations of the nucleon source and sink, respectively.

In addition to the connected contribution, another type of diagram also exists except in the isovector limit. This type of diagram is shown in Figure 5, and is called the disconnected diagram. We are not considering this in most of our calculations, and only investigate it in our algorithmic development phase.

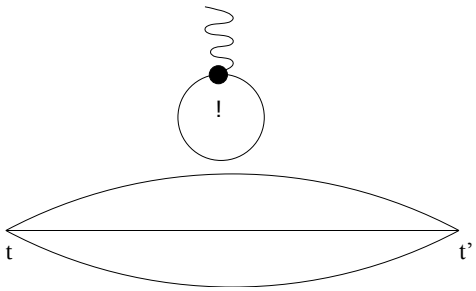

Figure 5: An illustration of the disconnected contribution to the nucleon three-point functions. t and t' are the locations of the nucleon source and sink, respectively.

In recent years, there have been a lot of efforts in reducing the computational cost and making efficient use of the computing resources. Below we list a few algorithmic improvements that we have used in this project.

a) Simultaneous Multiple Sequential Propagators

Because every physical observable has to be gauge invariant, any gauge-variant contractions will vanish over a large, statistically independent, gauge ensemble. This property leads to the so-called "coherent-sink trick" [12,13], in which sequential propagators for different forward propagators can be computed simultaneously. If we have a three-point function constructed from a forward propagator and an independently calculated sequential propagator from that forward propagator, the contraction looks like Figure 6(a). When multiple sequential propagators are calculated at the same time, in addition to the diagram in Figure 6(a), we will also have diagrams like Figure 6(b), where the red lines are contaminations from the other source x_1. Note that the blue line is in no way connected to the red lines, as they come from different sources. Hence this diagram is not gauge invariant, and should average to zero over a large gauge ensemble.

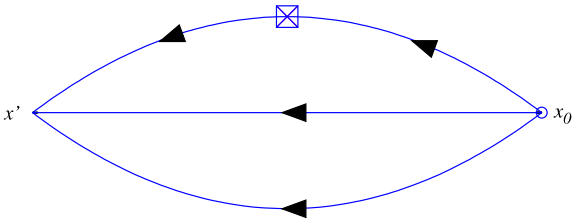

(a)The usual nucleon three-point contraction from a forward propagator and an independently calculated sequential propagator.

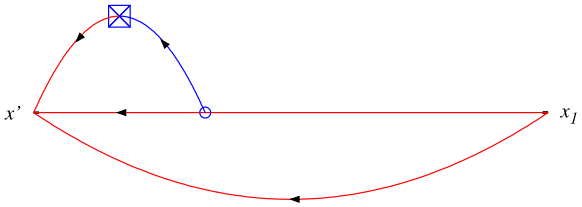

(b)The contamination from the other source to the nucleon three-point function with the *coherent-sink* method. The red lines are propagators from the other source(s).

Figure 6: Contributions to the nucleon three-point correlation functions.

With this method, the cost reduced is proportional to the number of sources used. In the past, we have employed this method for our calculations with four sources per gauge configuration. This leads to a factor of 4 reduction in computation time for the sequential propagators.

b) Mobius-Accelerated Domain Wall Inverter

We have also incorporated an improved code to do the matrix inversions. Specifically, instead of using double precision for the entire iterative process to obtain the matrix inversion, we can use single precision at the beginning of the iterative process and only impose double precision at the end to get the solution in double precision. Another improvement we have implemented is to use a less expensive Mobius domain wall formulation, which requires a smaller extent in the fifth dimension to achieve the same level of chiral symmetry breaking, to generate the initial guess for the domain wall fermion formulation we are using. The combination of such improvements results in the Mobius-Accelerated Domain Wall Inverter [14], which makes the matrix inversions twice as fast.

c) All-Mode Averaging (AMA)

While the calculations described above form the framework of our project, brute force calculations are not sufficient to reduce the statistical errors on

computed, physical, quantities to the ~ 5% level, or below, necessary to test the theory and experiment. To get to this level, especially for the 170 MeV pion mass ensemble, so-called all-mode averaging (AMA) [15] is needed. AMA requires the computation of the lowest eigenmodes of the Dirac operator and corresponding eigenvectors of the Dirac operator in order to construct the low-mode part of the quark propagator, S_l, and then the part of correlation function, O_l, is constructed from S_l. The high-mode part of the observable can be approximated with sloppy CG (conjugate gradient with a relaxed stopping condition of the order of 1e-3, instead of the typical *1e-8* in the conventional calculations). So the original observable O is divided into the approximate part, O_{appr} and the correction part, O_{rest}, so that $O = O_{appr} + O_{rest}$.
Since the statistical ensemble has the invariance under the translational invariance G due to the symmetry of the action used, and the construction of O_{appr} is covariant under G, the following equation for the statistical average under the observable $\langle O \rangle$ holds: $\langle O_{appr} \rangle = \langle O^G_{appr} \rangle$, where $\langle O^G_{appr} \rangle$ is the observable under the symmetry transformation G. The ensemble average for the observable $\langle O \rangle$ can now be determined as

$$\langle O \rangle = \langle O_{AMA} \rangle + \langle O_{rest} \rangle,$$

where $O_{AMA} = \frac{1}{N_G} \sum_G O^G_{appr}$ is the all-mode-averaging part of the observable O averaged over N_G symmetry transformations with sloppy CG. Since translation is a symmetry in our action, G can be taken to be just the shift of the lattice coordinates, allowing us to average the correlation functions over the entire four-volume of the lattice and increase the statistics significantly with negligible extra computing cost once the low eigenmodes have been calculated.

To correct for the bias in $\langle O_{AMA} \rangle$ due to sloppy CG, $\langle O_{rest} \rangle$ needs to be determined. We do this by performing (much fewer) exact calculations on the same gauge configuration, such that

$$O_{rest} = \frac{1}{N_{exact}} \sum O_{exact} - \frac{1}{N_G} \sum_G O^G_{appr}.$$

Note that N_{exact} is typically of O(1), while N_G is of O(100).

2.2 Usage Status

As of today (March 4, 2014), we have only used 1.9% of the requested time of 8242560.0 core hours. As we will explain further in Section 7, due to our shifted focus to the calculation with physical pion masses, we were not able to use the RICC resources, as the new calculation has much higher demand on the memory capacity.

3. Results

This past year's main development was the application of the All-Mode-Averaging (AMA) in the calculation of nucleon structure. Because O(1000) 5-dimensional eigenvectors are needed in AMA, which require at least 10 Terabytes of memory in the calculation, we performed all the AMA calculations on the Gordon supercomputer located at San Diego Supercomputing Center through our allocation with XSEDE. Gordon has a larger memory per core, and makes our memory-intensive AMA calculations feasible. We have added the results with a shorter source-sink separation to study the excited-state contaminations. Our much improved results have been presented in two talks at the 31 International Symposium on Lattice Field Theory.

3.1 The Benefits of AMA

In the implementation for the nucleon calculations presented here, we first computed 1000 low-lying eigenmodes of the DWF Dirac operator, and then use these low eigenmodes to compute the low-mode part of the propagator. The low-mode-deflated quark propagator is then computed to a *sloppy* stopping condition of order 10^{-3}, giving an approximate quark propagator, from which the approximate nucleon correlation functions are constructed. The approximate calculations were done on 7 time slices and 16 spatial source locations oneach time slice, giving a total of 112 measurements per configuration. The exact calculations were done on 4 time slices, with one spatial source location per time slice.

To further reduce the cost, we use the Möbius domain wall fermion operator in the approximate calculations with a smaller L_s= 16. The parameters of the Möbius DWF operator were chosen such that the valence residual mass roughly matches that in the dynamical simulation with the standard Shamir DWF operator.

In Figure 7 we show the comparison of the exact, approximate and all-mode-averaged results for the plateau of the isovector nucleon Dirac form factors at the first non-zero momentum (Figure 7(a)) and for the isovector Dirac form factors at different momentum transfers (Figure 7(b)).

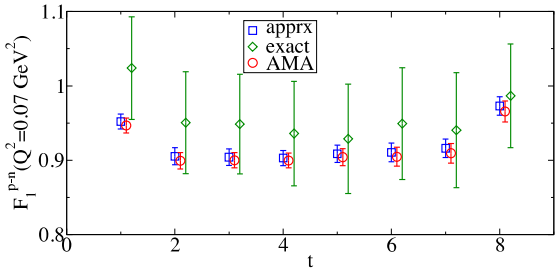

(a) Plateau of F_1^{p-n} at the first non-zero momentum with $M_\pi = 170$ MeV. Points are shifted slightly for clarity.

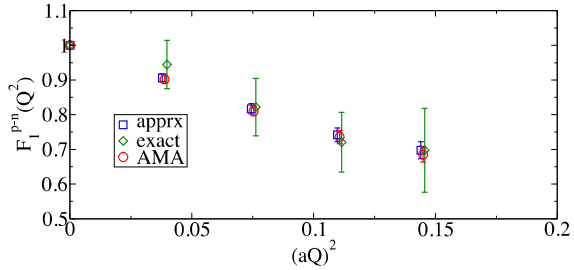

(b) Isovector Dirac form factor, $F_1^{p-n}(Q^2)$, with $M_\pi = 170$ MeV. Points are shifted slightly for clarity.

Figure 7: Comparison of the exact, approximate and all-mode-averaged results on the light ensemble with a pion mass of about 170 MeV.

The statistical errors are reduced by a factor of 4.6 to 6.4 over the whole Q^2 range (Figure 7(b)). Näively this would require a factor of 21 to 41 more computations if no improvements were implemented. As one sloppy calculation costs roughly about 1/65 of one exact calculation, taking into account the cost of the eigenmodes, the actual AMA cost is only 1.4 times that of the exact calculation without deflation. In this example, the speedup with AMA is 15 to 29 times.

3.2 Studies of Excited-state Contaminations

AMA also allows us to generate nucleon three-point functions with different source-sink separations without much additional cost, since we can reuse the eigenmodes that we calculated at the beginning. We studied the possible excited-state contaminations on the light ensemble with $M_\pi = 170$ MeV by comparing the plateaus of the nucleon Dirac and Pauli form factors at the source-sink separations of 7 and 9 lattice units, corresponding to roughly 1 fm and 1.3 fm physical separations, respectively. For $T = t_{snk} - t_{src} = 7$, eight configurations were used with 32 measurements per configuration. The comparisons of the plateaus for the isovector Dirac and Pauli form factors, $F_1^{p-n}(Q^2, t)$ and $F_2^{p-n}(Q^2, t)$, at two representative Q^2 values in each case are shown in Figure 8(a), from which we see no apparent excited-state contaminations. Fitting from $t = 3$–6 for $t_{snk} - t_{src} = 9$ and $t = 3$–4 for $t_{snk} - t_{src} = 7$, we obtain the results for $F_1^{p-n}(Q^2)$ and $F_2^{p-n}(Q^2)$ as shown in Figures 8(b) and 8(c). The lack of excited-state contaminations in our calculations may be attributed to the tuning of our nucleon source operator, which turns out to have a very good overlap with the nucleon ground state. It is possible that with increased statistics, the two source-sink separations may show statistically different results. But with the statistics available to us, we cannot identify any excited-state contaminations. This observation also drove our decision not to perform the calculation at a larger source-sink separation of T=11 as proposed.

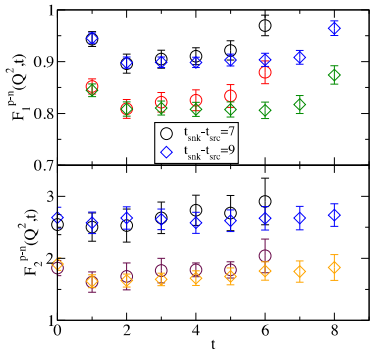

(a) Comparison of plateaus.

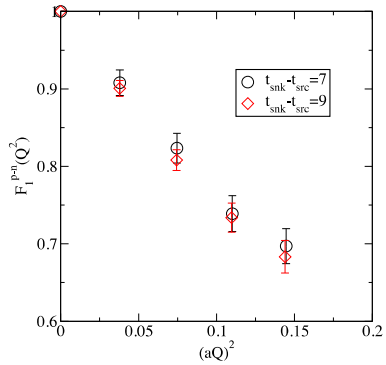

(b) Comparison of $F_1^{p-n}(Q^2)$.

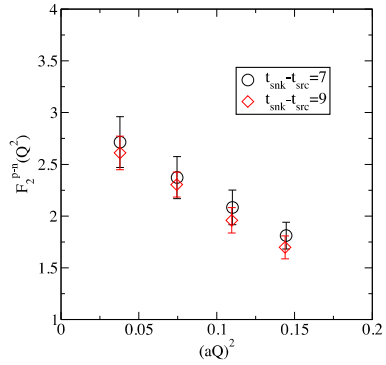

(c) Comparison of $F_2^{p-n}(Q^2)$.

Figure 8: Comparison of results with two different source-sink separations at $M_\pi = 170$ MeV.

Similarly, we observed no excited-state contaminations for the nucleon axial charge. In Figure 9 we present jackknife difference of the two source-sink separations for the four isovector quantities, the isovector vector charge, g_V, and the axial charge, g_A. The solid red symbols are the differences for the eight configurations where both separation calculations exist. The faded symbols are the values of the observables themselves in this range of trajectories, red with the longer and blue the shorter separations, respectively.

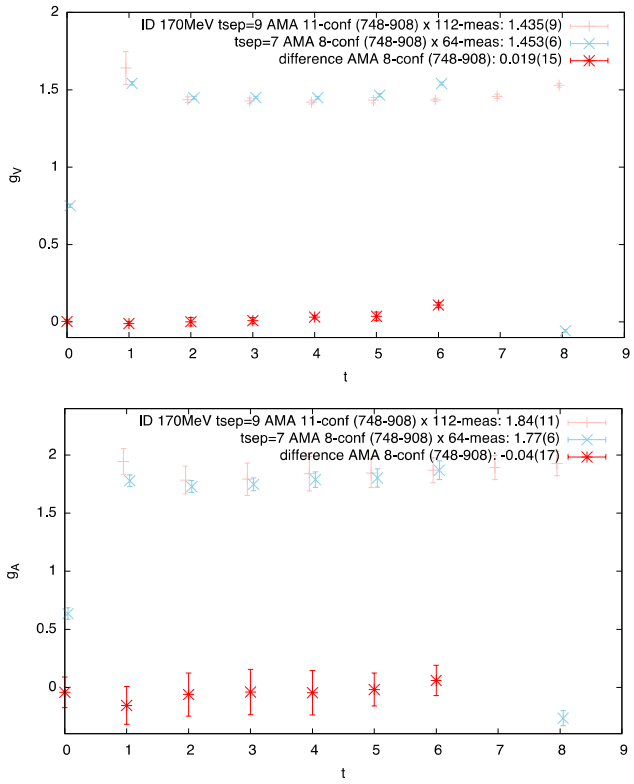

Figure 9: Comparison of two source-sink separations, 7 and 9 lattice units, or 1.0 and 1.3 fm: Jack- knifed differences between the two separations (solid red symbols) fail to show any sign of excited-state contamination in any of the observables, the isovector vector charge, g_V and the axial charge, g_A.

3.3 Results

3.3.1 Nucleon Vector Form Factors

Our results for the isovector Dirac and Pauli form factors can be fit with the empirical dipole form, from which we obtain the results for the isovector Dirac radius, Pauli radius and the anomalous magnetic moment. These results, together with the previous calculations with 2-flavor [8] [16] and 2+1-flavor [8] domain wall fermions, are shown in Figure 10. We also show the comparison between the 2012 results without AMA (brown empty diamonds) and this year's improved results (red filled diamonds). It is clear that AMA has offered substantial error reduction in the calculations with M_π = 170 MeV. While the results for the isovector Pauli radius and the anomalous magnetic moment are within two standard deviations of the experimental values at M_π = 170 MeV, the isovector Dirac radius still shows a 20% deficit. In Ref. [11], the authors found that excited-state contaminations tend to result in a smaller value for the Dirac radius. Since we observed no excited-state contaminations as discussed in the previous section, the deficit here may be due to a large chiral log near the physical pion mass.

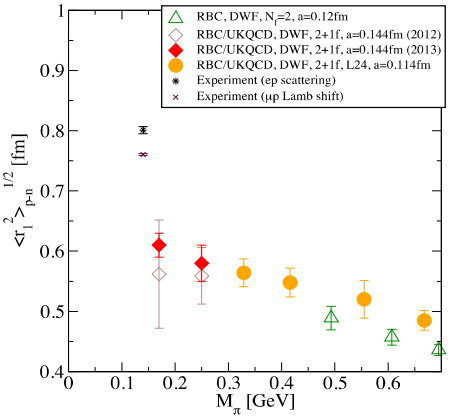

(a)

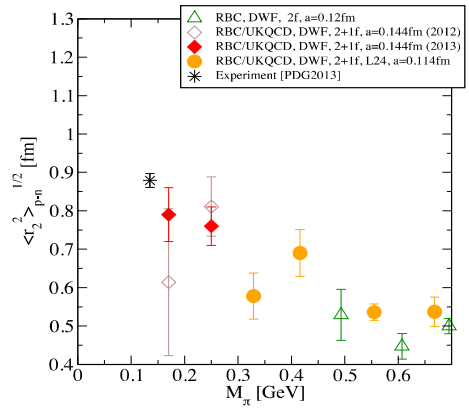

(b)

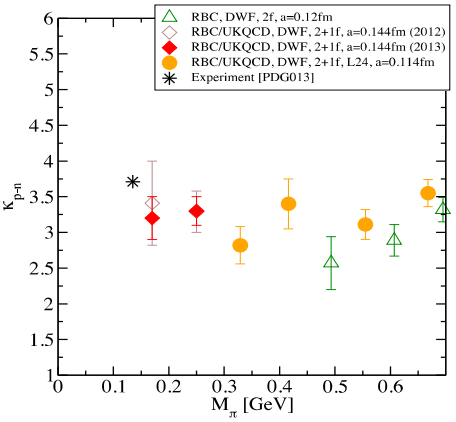

(c)

Figure 10: Preliminary results for isovector nucleon (a) Dirac radius, (b) Pauli radius and (c) anomalous magnetic moment.

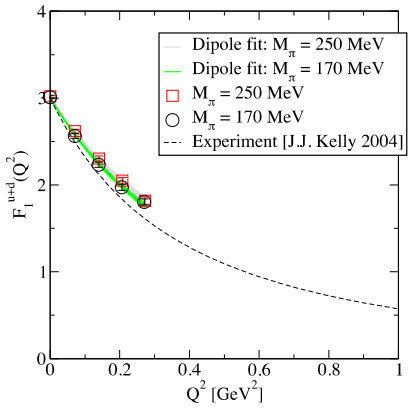

(a)

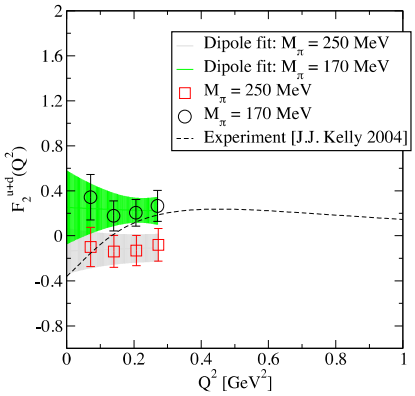

(b)

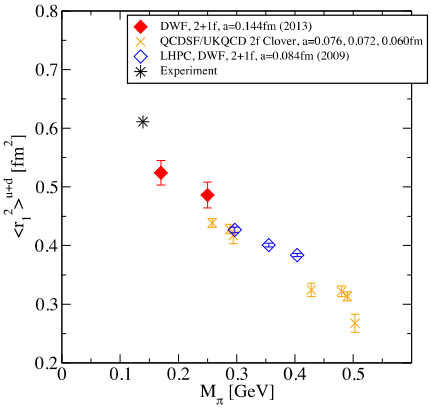

(c)

Figure 11: Connected contribution to the isoscalar nucleon (a) Dirac form factors, (b) Pauli form factors and (c) the Dirac radius. The dashed lines are the parameterizations of the experimental data in Ref. [17].

While we did not include disconnected diagrams in our calculations, we can still look at the contribution of the connected diagrams to the isoscalar Dirac and Pauli form factors, shown in Figure 11(a) and Figure 11(b) respectively. The shaded curves are from dipole fits. While $F_1^{u+d}(Q^2)$ fits well to the dipole form and allows us to determine the isoscalar Dirac radius, $F_2^{u+d}(Q^2)$ shows little curvature and the extracted values for the radius and anomalous magnetic moment are consistent with zero. In Figure 11(c) we show our results for the isoscalar Dirac radius, together with two other lattice calculations [18,19]. As opposed to the isovector case, here our result for the isoscalar Dirac radius at M_π = 170 MeV approaches the experiment steeply.

3.3.2 Nucleon Axial Charge

In Figure 12 we plot our recent calculations of g_A/g_V against pion mass squared, m_π^2, at the top, and against the finite-size scaling parameter, $m_\pi L$, at the bottom. The solid and faded red symbols denote results from earlier gauge ensembles in a $24^3\times64$ lattice volume, and solid and faded blue from the DSDR ensembles with pion masses 170 MeV and 250 MeV. The solid symbols are with the enhanced statistics this year, and faded ones are from our earlier calculations.

We note the latest four calculations with improved statistics show no sign of approaching the experiment as the pion mass is set light, down to as light as about 170 MeV. This behavior does not motivate us to fit them for any pion mass dependence. About 10-% deficit from the experiment is persistent down to this mass which is very close to physical, indicating there may be a large chiral log as the pion mass approaches the physical limit or there may be other large systematic effects. We also note these results of ours are consistent with almost all the recent calculations of the quantity using various different actions, lattice spacings, and spatial volumes.

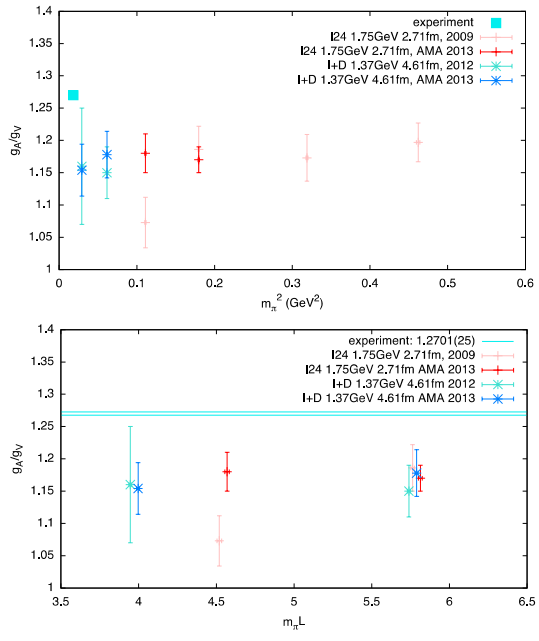

Figure 12: Dependence the nucleon axial charge on the pion mass squared, m_π^2, and the product of the pion mass and the lattice spatial extent, $m_\pi L$.

4. Conclusion

AMA offers substantial speedup in terms of computational efficiency in the calculation of nucleon structure as reported here. Our studies on the possible excited-state contributions to the nucleon ground-state quantities indicate no statistically significant contaminations, and our choice of T=9 is sufficient to suppress the excited-state contributions at this statistical level. However, our results for both the nucleon radii and the nucleon axial charge still show significant deficits from the experimental values, even with a pion mass of 170 MeV, which is very close to the physical pion mass of 135 MeV. It is thus very important and scientifically interesting to perform the calculations directly at the physical pion mass, which is an ongoing effort.

5. Schedule and prospect for the future

We have finished the calculations on these gauge configurations, and are in the process of publishing a journal article. Building upon the success of the calculations presented here, currently there is an ongoing effort in performing the calculations directly at the physical pion mass with two different lattice spacings, once again with the AMA technique that is first applied on the DSDR ensembles. These calculations at the physical pion mass will eliminate the needs to perform chiral extrapolations, and the two lattice spacings will give us an idea of the size of the lattice discretization effects.

6. If you have a "General User" account and could not complete your allocated computation time, specify the reason.

The reasons we did not complete the allocated computation time are listed below:

- The final analysis of the two source-sink separations indicates that the excited-state contaminations with T=9 are already negligible given the statistics accessible to us. We did not see the need to perform the calculation with an even larger, T=11, source-sink separation, as originally proposed.
- Since we switched to AMA, the memory requirement to store all the necessary eigenvectors is too great to fit into the RICC system. Instead, we performed the AMA part of the calculations on the Gordon supercomputer based in San Diego, US. Gordon offers 4 GB memory per core, and is more suitable for our calculations.
- With the availability of 2+1-flavor gauge ensembles with domain wall fermions at the physical pion mass, we have shifted our focus to the calculations on these gauge ensembles. The gauge ensembles have lattice volumes of $48^3\times96$ and $64^3\times128$, which are substantially larger than the $32^3\times64$ lattices we have performed the calculations on. The increase of the lattice volumes makes it even more impractical to carry out the calculations on the current RICC system.

References:

[1] K. G. Wilson, Phys. Rev. **D10**, 2445 (1974).

[2] J. Gasser and H. Leutwyler, Ann. Phys. **210**, 142 (1984).

[3] C. R. Allton, D. J. Antonio, Y. Aoki, T. Blum, P. A. Boyle, N. H. Christ, and M. A. Clark, Phys. Rev. **D78**, 114509 (2008).

[4] Y. Shamir, Nucl. Phys. **B406**, 90 (1993).

[5] T. Blum, P. Chen, N. Christ, C. Cristian, C. Dawson, G. Fleming, and Others, Phys. Rev. **D69**, 74502 (2004).

[6] T. Blum and others, Phys. Rev. **D66**, 14504 (2002).

[7] RBC Collaboration, UKQCD Collaboration, R. Arthur, T. Blum, P. A. Boyle, N. H. Christ, N. Garron, R. J. Hudspith, T. Izubuchi, C. Jung, C. Kelly, A. T. Lytle, R. D. Mawhinney, D. Murphy, S. Ohta, C. T. Sachrajda, A. Soni, and J. M. Zanotti, 95 (2012).

[8] T. Yamazaki and others, Phys. Rev. **D79**, 114505 (2009).

[9] T. Yamazaki, Y. Aoki, T. Blum, H. Lin, M. Lin, S. Ohta, S. Sasaki, R. Tweedie, and J. Zanotti, Phys. Rev. Lett. **100**, 171602 (2008).

[10] Y. Aoki, T. Blum, H.-W. Lin, S. Ohta, S. Sasaki, R. Tweedie, J. Zanotti, and T. Yamazaki, Phys. Rev. D **82**, 14501 (2010).

[11] J. R. Green, M. Engelhardt, S. Krieg, J. W. Negele, A. V Pochinsky, and others, arXiv Prepr. 1209.1687 (2012).

[12] J. D. Bratt, R. G. Edwards, M. Engelhardt, G. T. Fleming, M. F. Lin, H. B. Meyer, B. Musch, J. W. Negele, K. Orginos, A. V Pochinsky, M. Procura, D. B. Renner, D. G. Richards, W. Schroers, S. Syritsyn, and others, Proc. Sci. **LAT2008**, 141 (2008).

[13] J. D. Bratt, R. G. Edwards, M. Engelhardt, P. Hagler, H.-W. Lin, M. Lin, H. B. Meyer, and B. Musch, Phys. Rev. D **094502**, 1 (2010).

[14] H. Yin and R. D. Mawhinney, PoS **LATTICE201**, 51 (2011).

[15] T. Blum, T. Izubuchi, and E. Shintani, Phys. Rev. D **88**, 094503 (2013).

[16] H.-W. Lin, T. T. Blum, S. Ohta, S. Sasaki, and T. Yamazaki, Phys. Rev. D **78**, 14505 (2008).

[17] J. J. Kelly, Phys. Rev. **C70**, 68202 (2004).

[18] S. N. Syritsyn, others, J. D. Bratt, M. F. Lin, H. B. Meyer, J. W. Negele, a. V. Pochinsky, M. Procura, M. Engelhardt, P. Hagler, T. R. Hemmert, and W. Schroers, Phys. Rev. D **81**, 34507 (2009).

[19] S. Collins, M. Göckeler, P. Hägler, R. Horsley, Y. Nakamura, a. Nobile, D. Pleiter, P. E. L. Rakow, a. Schäfer, G. Schierholz, W. Schroers, H. Stüben, F. Winter, and J. M. Zanotti, Phys. Rev. D **84**, 074507 (2011).

Fiscal Year 2013 List of Publications Resulting from the Use of RICC

[Proceedings, etc.]

1. M. Lin, Nucleon form factors with 2+1 flavors of domain wall fermions and All-Mode-Averaging, arXiv:1401.1476 [hep-lat], PoS LATTICE2013 (2013) 275.
2. S. Ohta, Nucleon axial charge in 2+1-flavor dynamical DWF lattice QCD, arXiv:1309.7942 [hep-lat], PoS LATTICE2013 (2013) 274.

[Oral presentation at an international symposium]

1. M. Lin, "Nucleon form factors with 2+1 flavors of domain wall fermions and All-Mode-Averaging", The 31st International Symposium on Lattice Field Theory, Mainz, Germany, July 29 – August 3, 2013.
2. S. Ohta, "Nucleon axial charge in 2+1-flavor dynamical DWF lattice QCD", The 31st International Symposium on Lattice Field Theory, Mainz, Germany, July 29 – August 3, 2013.

[Others: Invited Talks]

1. S. Ohta, "Finite-size scaling of nucleon axial charge in domain-wall lattice QCD", JPS Meeting, Hiroshima University, Japan, March 26 – 29, 2013.
2. T. Izubuchi, "Lattice QCD and the HEP Intensity Frontier", Lattice QCD Computational Science Workshop, Oak Ridge National Laboratory, TN, April 29, 2013.
3. T. Izubuchi, "Nucleon Structure by Lattice QCD", PHENIX Workshop on Physics Prospects with Detector and Accelerator Upgrades, RIKEN, Wako, Japan, July 29, 2013.
4. S. Ohta, "Nucleon structure from 2+1-flavor domain-wall lattice QCD at nearly physical pion mass", JPS Meeting, Kochi University, September 20 – 23, 2013.
5. S. Ohta, "Nucleon structure from 2+1-flavor domain-wall lattice QCD at nearly physical pion mass", RIKEN Lunch Seminar, Brookhaven National Laboratory, Upton, New York, November 14, 2013.
6. M. Lin, "Nucleon Structure on the Lattice", High Energy Theory/RIKEN Lunch Seminar, Brookhaven National Laboratory, Upton, New York, March 28, 2014.
7. T. Izubuchi, "Study of nucleon structure by lattice QCD", JPS Meeting Invited Talk, Tokai-daigaku, Kanagawa, Japan, March 30, 2014.